SPE 105378

Multi-physics and Multi-scale Methods for Modeling Fluid Flow Through Naturally-Fractured Vuggy Carbonate Reservoirs

Peter Popov, Linfeng Bi, Yalchin Efendiev, Richard E. Ewing and Guan Qin, Institute for Scientific Computation, Texas A&M University, College Station, Texas 77843, USA; Jianglong Li and Yulin Ren, Exploration and Production Research Institute, China Petroleum & Chemical Corporation, Beijing, P.R. China 100083

This paper was prepared for presentation at the 15th SPE Middle East Oil & Gas Show and Conference held in Bahrain International Exhibition Centre, Kingdom of Bahrain, 11–14 March 2007.

Abstract

We present a novel approach for flow simulations through naturally-fractured vuggy carbonate reservoirs. This approach generalizes upscaling methods which have been successfully used to perform reservoir simulations on geological (fine) scales. Typically, vugular porous media is described using both Stokes and Darcy's equations at the fine-scale. We propose the use of simplified model based on Stokes-Brinkman equations. Stokes and Darcy equations can be obtained from these equations by appropriate choice of parameters. Moreover, in the presence of damaged zones between vugular regions and Darcy regions, Stokes-Brinkman equations allow a seamless transition.

The upscaling of fine-scale equations is addressed within homogenization theory. Appropriate local problems are solved to compute the effective permeabilities, which are further used for the simulations on the field scale. We present numerical results for homogeneous and heterogeneous background permeability fields. Our results show that the coarse-scale permeability field is greatly affected when the background permeability is heterogeneous. This is due to the fact that the high flow channels connecting some of the vugs significantly alter the upscaled permeability. We compare the coarse-scale pressure obtained from upscaled equations with the averaged fine-scale pressure. The results are in agreement which indicates that the upscaled models are accurate for practical purposes.

1. Introduction

Subsurface flows, as they occur in the production of hydrocarbons, are affected by heterogeneities in a wide range of length scales. The flow and transport of multi-phase flows are further complicated due to the presence of vugs. The geometries, locations and connectivities of vugs greatly affect the flow in reservoirs. The connectedness of the vugs can create high flow channels which significantly change oil production.

Because of the large uncertainties in the locations and geometries of the vugs, it is very difficult to numerically resolve the flow and transport through such systems. Thus, some type of upscaling or coarsening is needed to simulate flow and transport processes through vugular heterogeneous porous media. The main idea of upscaling techniques is to form coarse-scale equations with some prescribed analytical form that may differ from the underlying fine-scale equations. Our objective in this paper is to address the upscaling of flow through heterogeneous vugular media.

Typically, vugular porous media is described using both Stokes' and Darcy's equations at the fine-scale. In this paper, we propose the use of Stokes-Brinkman equations for fine-scale simulation. Stokes-Brinkman equations can be reduced to Stokes or Darcy equations by appropriate choice of the parameters. Moreover, in the presence of damaged zones between vugular regions and Darcy regions, Stokes-Brinkman equations allow a seamless transition. Due to uncertainties associated with interface locations between vugs and the rock matrix, Stokes-Brinkman equations introduce a somewhat coarse model that does not require precise interface locations and avoid local grid refinement issues that are needed near the interfaces.

To upscale flow through vugular regions is an important topic and addressed in previous findings (see e.g., Arbogast et al. [1,2]). Arbogast et al. use the homogenization theory and show that the coarse-scale equations are described by Darcy's law. The authors present a procedure for the computation of effective permeabilities. Our approach shares similarities with that of Arbogast et al. Arbogast et al. [1] use the coupled Darcy and Stokes equations at the fine-scale. In the context of Stokes-Brinkman equation, one can also obtain the homogenized equations for the regions with enclosed vugs. In a manner similar to that of Arbogast et al. [1], it can be shown that the upscaled equations are governed by Darcy's law. Moreover, the upscaled permeabilities can be computed using the solutions of the local problems. The upscaled quantities are greatly affected by the vug geometries and locations. For vugs that are connected, the upscaled permeability can be high and in this case, most of the flow is through vugular regions. We consider isolated vugs within a heterogeneous permeability background. In this case, the interaction between permeability field and vugs plays a crucial role in the calculation of upscaled permeabilities. Vugs that are isolated in low permeability regions, may not yield high effective permeabilities. On the other hand, vugs which are connected via high permeability channels lead to high effective permeability.

The effective permeability is further used to solve single-phase flow equations on the coarse-grid. We present several test examples, where the coarse-scale solution and the averaged fine-scale solution are compared. Our results show that the upscaled model produces accurate coarse-scale solution. In order to numerically solve the fine-scale problem, we employ a mixed finite element method and discretize the Stokes-Brinkman equations using Taylor-Hood elements.

The paper is organized as follows. In the next section, we discuss fine-scale equations. This is followed by presenting the upscaled equations in Section 3. Finally, in Section 4, we present several numerical examples, which include fine-scale numerical simulations, as well as computing effective permeability and coarse-level simulations.

2. Fine-scale equations

We consider the fluid flow in the region partly occupied with vugs. The flow equations within vugs are described by Stokes equations:

$$\begin{aligned} -\mu\Delta\mathbf{u} + \nabla p = 0 \\ \nabla\cdot\mathbf{u} = 0, \end{aligned} \tag{1}$$

where μ is the viscosity of the fluid, p is the pressure, and $\mathbf{u}$ is the velocity. The flow equations within the rock matrix are described by Darcy's law:

$$\begin{aligned} \mathbf{u} = -\mathbf{k}\nabla p \\ \nabla\cdot\mathbf{u} = q, \end{aligned} \tag{2}$$

where p is the pressure, $\mathbf{u}$ is the velocity field, q is the source term and $\mathbf{k}$ is the permeability tensor. Darcy's equation can be derived from Stokes equation using homogenization theory under the assumption of scale separation (see e.g., [1]). When Darcy's flow and Stokes flow are considered together, some interface conditions are needed for the well posedness of the problem. These conditions are well known (see e.g., [2,5,9,8]) and typically describe the continuity of the flux, normal stresses, and also impose certain restrictions on the tangential velocity field. More precisely, continuity of flux is given as

$$[\mathbf{u}\cdot n] = 0, \tag{3}$$

where $[\cdot]$ describes the jump. Continuity of the normal fluxes can be written as

$$2\mu D\mathbf{u}_f \cdot n \cdot n = p_f - p_d, \tag{4}$$

where $(D\mathbf{u})_{i,j} = \frac{1}{2}\left(\frac{\partial u_i}{\partial x_j} + \frac{\partial u_j}{\partial x_i}\right)$, p_f is the pressure in vugular region, p_d is the pressure in the rock matrix, and $\mathbf{u}_f$ is the velocity in vugular region. Finally, one also needs to impose corrections for tangential velocity field due to fluid flow from the rock matrix to vugular region. These relations are described by Beavers-Joseph-Saffman conditions [5,9,8].

In this paper, a somewhat unified and simplified approach is undertaken. In particular, the fine-scale equations are modeled using Stokes-Brinkman equations [6,4,3,10]:

$$\begin{aligned} \mu\mathbf{k}^{-1}\mathbf{u} + \nabla p - \mu^*\Delta\mathbf{u} = 0, \\ \nabla\cdot\mathbf{u} = 0 \end{aligned} \tag{5}$$

where μ^* is an effective viscosity. Note that by choosing $\mu^* = 0$ in the vugular region, equation (5) reduces to Darcy's law. On the other hand, by choosing $\mathbf{k} = \infty$ (or very large), (5) reduces to Stokes equations. Thus, one can obtain Stokes or Darcy's equations by suitable choices of the parameters μ^* and $\mathbf{k}$ by defining them in vugular and rock matrix regions, respectively.

In the porous region ($\mathbf{k} < \infty$) it is known [12] that for moderately small permeabilities and pore volume fractions, the diffusive term $\mu^*\Delta\mathbf{u}$, where μ^* takes values close to the fluid viscosity μ, intoroduces only a small perturbation of the velocity and pressure fields as compared to a pure Darcy law ($\mu^* = 0$). Thus, in our fine-scale model it is assumed $\mu^* = \mu$, where μ is the viscosity of the fluid. In the vugular (free flow) region one has $\mu^* = \mu$ and the permeability is taken to be infinite, thus eliminating the $\mu\mathbf{k}^{-1}\mathbf{u}$ term in (5) and reducing it to the Stokes equation (1). In Section 4, we present a numerical example which shows that the Stokes-Brinkman solution with the choice $\mu^* = \mu$ in the porous region is very close to the solution of coupled Stokes and Darcy equations.

The Stokes-Brinkman equations (5) and the coupled Stokes-Darcy system [1,2] are closely related. It can be shown (see e.g. [12] and the references therein) that by selecting values for μ^* in the porous region in the Sokes-Brinkman system (5), which are different from μ, one can introduce boundary layers at the rock/vugs interface. These boundary layers mimic the Beavers-Joseph-Saffman interface conditions for the coupled Stokes-Darcy equations. Thus, jump-like conditions for the tangential velocity component at the interface can also be prescribed via equations (5), by selecting an appropriate value for $\mu^* \neq \mu$. However, to make such a choice (or, equivalently, to select appropriate parameters for the Beavers-Joseph conditions in the context of coupled Stokes-Darcy equations) it is necessary to have either detailed knowledge of the porous microstructure of the rock, or extensive experimental data. Moreover, Beavers-Joseph interface conditions for coupled Stokes Darcy equations are most appropriate for flows tangential or almost tangential to the free flow/porous interface. In the case of disconnected vugs immersed in a porous rock, it is more reasonable to assume continuity of the velocity (both tangential and normal) for equations (5) where the choice $\mu^* = \mu$ in the porous region is appropriate. As the numerical simulations of Section 4 show, the flow tends to be mostly normal to the interface, for disconnected vugs transferring mass between the rock and the vug.

The use of the Stokes-Brinkman equations for the fine-scale model over the more traditional, coupled Stokes-Brinkman equations has certain advantages for vugular media. Typically, in vugular porous media, there are large uncertainties with the location of the boundaries of the vugs. Also, these boundary regions are often eroded compared to the interior of the rock. The Stokes-Brinkman equations allow us to have seamless transition between the rock and the vug by varying the permeability field close to the interface. Moreover, from a numerical point of view, it is easier to solve a monolithic system such as Stokes-Brinkman, in contrast to a coupled Darcy-Stokes system which requires an additional iterative scheme. Also, in the near interface region, Stokes-Brinkman equations allow us to avoid the typical grid refinement issues necessary for resolving the interface between Darcy and Stokes region.

3. Coarse-scale equations

In this section, we describe the coarse-scale equations. In particular, we will be interested in upscaling vugular regions that can be enclosed within coarse-block regions with heterogeneous permeability. It was shown in [2] that the upscaled equation in the case of coupled Darcy's and Stokes equation is Darcy's law. For Stokes-Brinkman fine-scale equations, it can be also shown that the upscaled equations are described by Darcy's equations, where the upscaled permeability strongly depends on the vugs and the background permeability field. The local problems are computed using

$$\begin{aligned} \mu \mathbf{k}^{-1}\mathbf{u} + \nabla p - \mu^* \Delta \mathbf{u} &= \xi, \\ \nabla \cdot \mathbf{u} &= 0 \end{aligned} \tag{6}$$

where ξ is unit body force and $\mu^* = \mu$. Equation (6) is subject to some boundary conditions (typically periodic). The boundary conditions do not play a significant role in computing the effective coefficients if there is a scale separation. We have tested periodic boundary conditions as well as no-flow type boundary conditions with unit pressure gradient. Given the solution of the local problem, the upscaled permeability is computed from

$$\mathbf{k}^* \xi = \langle \mathbf{u} \rangle,$$

where $\langle \ \rangle$ is the volume average over the coarse block. One can also choose the formulation based on dissipative energy.

Once the upscaled permeability is computed, the coarse-scale equations are solved in the global domain:

$$\begin{aligned} \mathbf{u} &= -\mathbf{k}^* \nabla p \\ \nabla \cdot \mathbf{u} &= q, \end{aligned} \tag{7}$$

where q is the source term. This approach shares similarities with multiscale approaches presented in [2]. In multiscale approaches, the basis functions are constructed using local solutions (6). Then these basis functions are coupled via global formulation of the problem. Multiscale approaches allow us to recover the fine-scale features of the velocity field. If (7) is written in a finite volume context, our approach computes the effective transmissibilities via local solutions. In this sense, our approach shares similarities with multiscale approaches. We are currently implementing the multiscale finite volume approach.

In the presence of large vugs, Stokes-Brinkman equations are used in the overall region, with corresponding upscaled permeabilities. One can also keep Stokes equations within large vugs. As is mentioned earlier, the interaction of vugs and background heterogeneities play a crucial role in the computation of upscaled permeabilities. This is more evident for enclosed vugs that are considered in this paper. If the vugs are surrounded by low permeability regions, then the vugs do not significantly alter the upscaled permeabilities. However, if vugs are connected via high permeability channels, then vugs can dramatically alter the overall upscaled permeability.

4. Numerical results

We now present numerical results. The systems considered are representative of cross sections in the subsurface. We will consider both homogeneous permeability background as well as heterogeneous permeability background. For simplicity, we set the system length L_x in the horizontal direction x to be the same as the formation thickness L_z; in the results presented below, $L_x/L_z = 1$. In the case of heterogeneous permeability fields, the fine grid permeability fields are realizations of prescribed overall variance (quantified via σ^2, the variance of $\log k$), correlation structure and covariance model. We consider models generated using GSLIB algorithms [7], characterized by spherical variogram. For the spherical variogram model, the dimensionless correlation lengths (nondimensionalized by L_x and L_z respectively) are designated l_x and l_z.

In order to numerically solve the fine-scale problem (5), as well as the cell problems (6) we use a mixed finite element method for the Stokes-Brinkman equations in the primary variables $\mathbf{u}$ and p. We use Taylor-Hood elements (continuous quadratic velocity and continuous linear pressure, for more details, see e.g. [11]) on unstructured triangular grids. The linear systems resulting from this finite element discretization are symmetric and indefinite. These are solved using preconditioned conjugate gradient method for the pressure schur complement. For more details on these types of numerical the reader is referred to [11].

Our first numerical example compares the solution of coupled Stokes and Darcy equations [1,2] with the solution of Stokes-Brinkman equations (5). In Fig.1, the velocity and streamlines are plotted for a single vug inclusion and homogeneous background permeability field using Stokes-Brinkman equations (5) with $\mu^* = \mu$. In Fig.2, the same quantities are plotted for the solution of coupled Stokes and Darcy equations. There is almost no difference in velocity fields. The latter justifies the use of Stokes-Brinkman equations with $\mu^* = \mu$. Note that one can always take μ^* to be sufficiently small to obtain Darcy's equation in the rock matrix region. The objective of these numerical examples is to show that we do not need to tune the parameter μ^*. In Fig.3 and Fig.4, we compare the pressure profiles for Stokes-Brinkman and coupled Stokes and Darcy equations. Because there is almost no difference between pressure fields, these results again suggest that $\mu^* = \mu$ can be used in our fine-scale model.

In the next set of numerical tests, we consider a representative elementary volume with a number of small vugs and homogeneous permeability background. The vugs are distributed randomly throughout the volume and the permeability field is taken to be $\mathbf{k} = 10^{-10}\mathbf{I}$ (in SI units, m^2), where $\mathbf{I}$ is the identity matrix. As for boundary conditions, we consider no flow at the top and bottom and zero Neumann for fluid stress at the inlet and outlet boundaries and unit body force in horizontal (x) direction. As the body force term can be absorbed into the pressure and vice versa (observe that $\nabla x = (1,0)$) and the viscous part of the fluid stress tensor x is orders of magnitude smaller then the pressure, these boundary conditions are equivalent to specifying a pressure drop of 1 between the left and right side of the domain and no body force. In Fig. 5, the velocity field (as well as streamlines) and pressure field are depicted. One can observe that the streamlines go through vugs which indicate that vugs represent high permeability regions. The upscaled permeability is computed for this representative elementary volume and is apprixametly 30% higher compared to the homogeneous, background permeability. The corresponding fine-scale solution of Stokes-Brinkman equation is plotted in Fig.5. This suggests that the presence of the vugs significantly increases the permeability.

In our next set of numerical experiments, we would like to solve the coarse-scale equations and compare the averaged fine-scale solution and the coarse-scale solution. Our first example is homogeneous isotropic background permeability field with randomly distributed ellipsoidal vugs. The boundary conditions from the previous example are used. First, we present the fine-scale solution in Fig. 6. On the left plot, the velocity field and the streamlines are plotted. On the right plot, the pressure field is plotted. Overall upscaled permeability is approximately 15% higher than the background permeability. Because of ellipsoidal shape of the vugs, we observe anisotropy in the upscaled permeability. We divide the whole domain into 5×5 coarse grid regions and in each region the upscaled permeability is computed. The results are plotted in Fig.7 for horizontal component of the permeability field (k_{11}). From this figure we observe that in the coarse regions with high concentration of vugs, the upscaled permeability is higher. In Figure 8, we plot the corresponding coarse-scale pressure. We have compared this coarse-scale pressure with the averaged coarse-scale pressure obtained from fine-scale solution. The L_2 relative error was found to be less than 2 % and there is no visual difference in the plots. For this reason, we do not present the plot of averaged fine-scale pressure field. This result suggests that the proposed upscaling method provides accurate coarse-scale solution for homogeneous background permeability field.

Our final set of numerical tests are devoted to the case with heterogeneous background permeability as partly shown in Fig. 10. The vug population (size, shape and locations) is identical to the previous example. However, the permeability field, shown in Fig.10, is variable. It has long correlation length in the horizontal direction ($l_x = 0.4$), smaller correlation length in the vertical direction ($l_z = 0.1$), and is generated using the spherical variogram as preciously discussed. The locations of the vugs are the same as those in Fig. 6. In Fig.9, the fine-scale solution is plotted for velocity and pressure fields. We see from this figure that the heterogeneous permeability field creates additional high flow channels for the vugs which can enhance connectivity of the media. This is more evident if one compares Fig.6 and Fig.9. The presence of the background heterogeneous permeability field alters the streamline significantly. Comparing Fig.7 and Fig.11, one can also observe that the upscaled permeabilities are quite different for homogeneous and heterogeneous background permeabilities. The highest permeability in the case of heterogeneous background permeability is $3.36*10^{-10}m^2$, while the highest permeability in the case of homogeneous background permeability is only $1.52*10^{-10}m^2$. Moreover, one can also observe different pattern structures in the graphs of upscaled permeabilities. The upscaled pressure is computed using upscaled permeabilities, and the result is depicted in Fig. 12. Again, we compared the upscaled pressure with averaged fine-scale pressure and the relative L_2 error is less than 5%. There is no visual difference between two plots. For this reason, we do not include the plot of averaged fine-scale permeability field. This result again suggests that the proposed upscaling method provides an accurate coarse-scale solution for heterogeneous background permeability field.

5. Discussion and Summary

The results of the previous section demonstrate that a simplified fine-scale model based on Stokes-Brinkman equations can be used to describe the flow through vugular porous media. Our upscaled results show that the heterogeneous background permeability field can give very different results compared to homogeneous background permeability with the same vug locations. In particular, the presence of high permeability channels connecting the vugs can increase substantially the overall permeability. The numerical tests show that the proposed upscaling is accurate and can be used in practice for upscaling of flow through vugular porous media.

Nomenclature

$\mathbf{k}$	Permeability tensor
l	Correlation length
L	Length
p	Pressure
q	Source term
$\mathbf{u}$	Velocity
μ	Viscosity
σ^2	Variance of $\log(k)$
$\mathbf{I}$	Identity tensor

Superscripts

$*$ upscaled or effective quantity

6. Acknowledgement

We greatly appreciate the support of SINOPEC. YE would like to acknowledge the support of DOE. We are also grateful to Dr. Oleg Iliev from Fraunhofer ITWM, Kaiserslautern, Germany, for his insightful suggestions and comments.

References

[1] T. ARBOGAST AND D. S. BRUNSON, *A computatonal method for approximating a darcy-stokes system governing a vuggy porous medium*, (2006). submitted.
[2] T. ARBOGAST AND H. L. LEHR, *Homogenization of a darcy-stokes system modeling vuggy porous media*, omputational Geosciences, (2006). to appear.
[3] J.-L. AURIAULT, C. GEINDREAU, AND C. BOUTIN, *Filtration law in porous media with poor separation of scales*, Transp. Porous Media, 60 (2005), pp. 89–108.
[4] J. BEAR, *Dynamics of Fluids in Porous Media*, Elsevier, 1972.
[5] G. BEAVERS AND D. D. JOSEPH, *Boundary conditions at a naturally permeable wall*, J. Fluid Mech., 30 (1967), pp. 197–207.
[6] H. C. BRINKMAN, *A calculation of the viscous force exerted by a flowing fluid on a dense swarm of particles*, Appl. Sci. Res., A1 (1948), pp. 27–34.
[7] C. V. DEUTSCH AND A. G. JOURNEL, *GSLIB: Geostatistical software library and user's guide, 2nd edition*, Oxford University Press, New York, 1998.
[8] W. JÄGER AND A. MIKELIC, *On the interface boundary condition of Beavers, Joseph, and Saffman*, SIAM J. Appl. Math., 60 (2000), pp. 1111–1127 (electronic).
[9] P. G. SAFFMAN, *On the boundary condition at the interface of a porous medium*, Studies in Applied Mathematics, 1 (1971), pp. 93–101.
[10] E. SÁNCHEZ-PALENCIA, *Homogenization method for the study of composite media*, in Asymptotic analysis, II, vol. 985 of Lecture Notes in Math., Springer, Berlin, 1983, pp. 192–214.
[11] S. TUREK, *Efficient Solvers for the incompressible flow problems: an algorithmic and computational approach*, Springer, 1999.
[12] V. LAPTEV, *Numerical solution of coupled flow in plain and porous media.* PhD Dissertation (2003), Technical University of Kasierslautern.

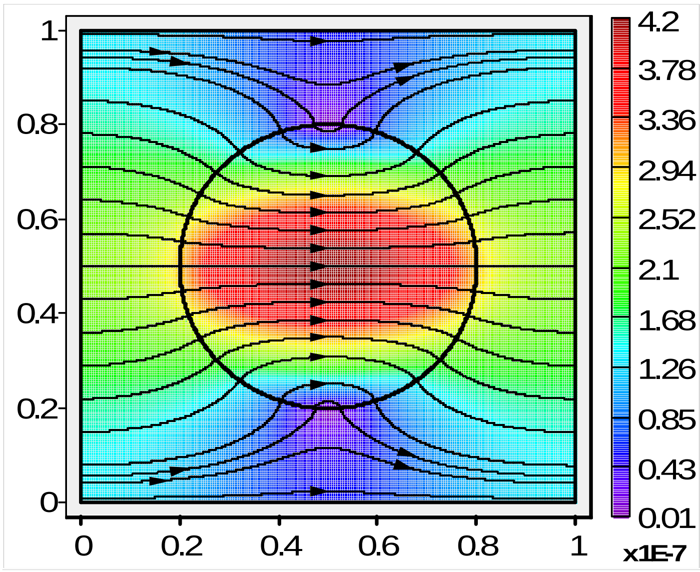

Figure 1. Velocity and streamlines for a single vuggy inclusion. Periodic boundary conditions.

Properties: $\mathbf{k}=10^{-10}m^2$, $\mu=0.001Pa\cdot s$ (water), $\mu^*=\mu$.

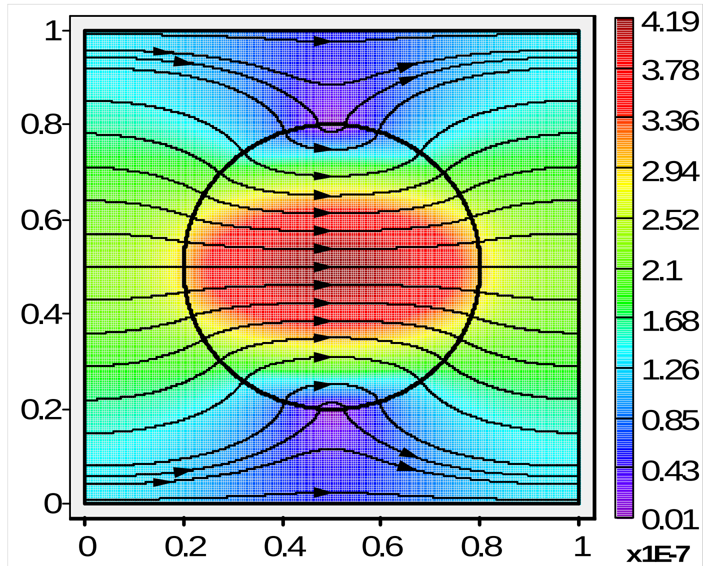

Figure 2. Velocity and streamlines for a single vuggy inclusion. Periodic boundary conditions.

Properties: $\mathbf{k}=10^{-10}m^2$, $\mu=0.001Pa\cdot s$ (water). Coupled Stokes and Darcy equations.

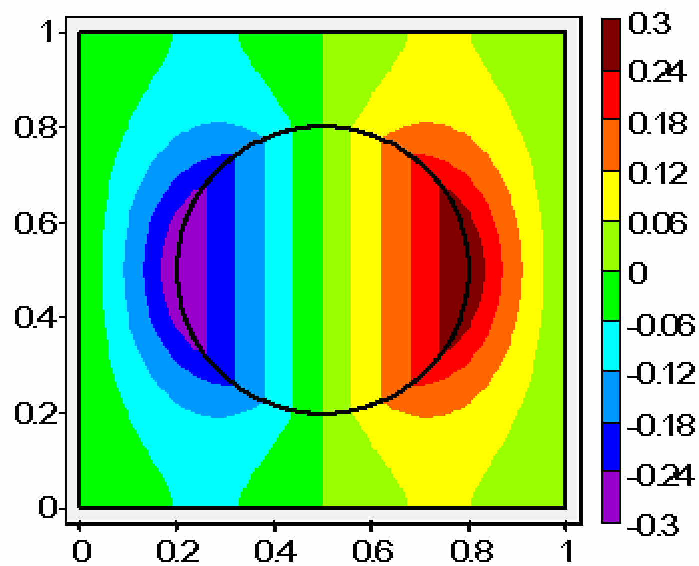

Figure 3. Pressure for a single vuggy inclusion. Periodic boundary conditions.

Properties: $\mathbf{k}=10^{-10}m^2$, $\mu=0.001Pa\cdot s$ (water), $\mu^*=\mu$.

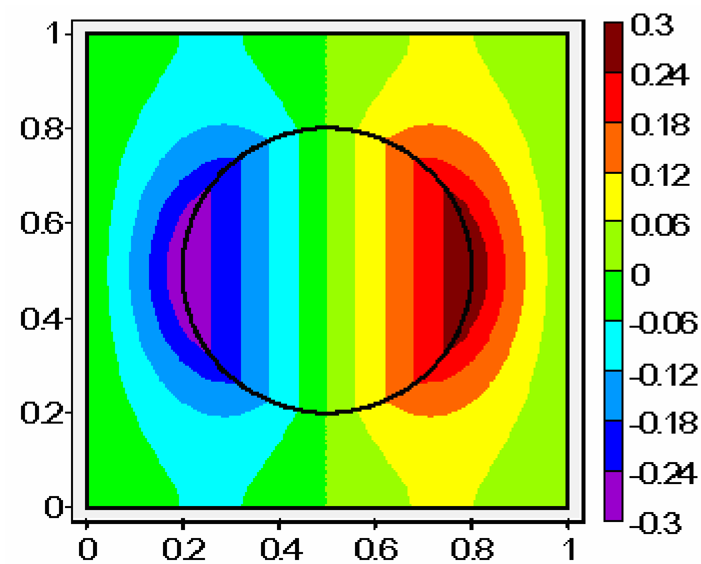

Figure 4. Pressure for a single vuggy inclusion. Periodic boundary conditions.

Properties: $\mathbf{k}=10^{-10}m^2$, $\mu=0.001Pa\cdot s$ (water). Coupled Stokes and Darcy equations.

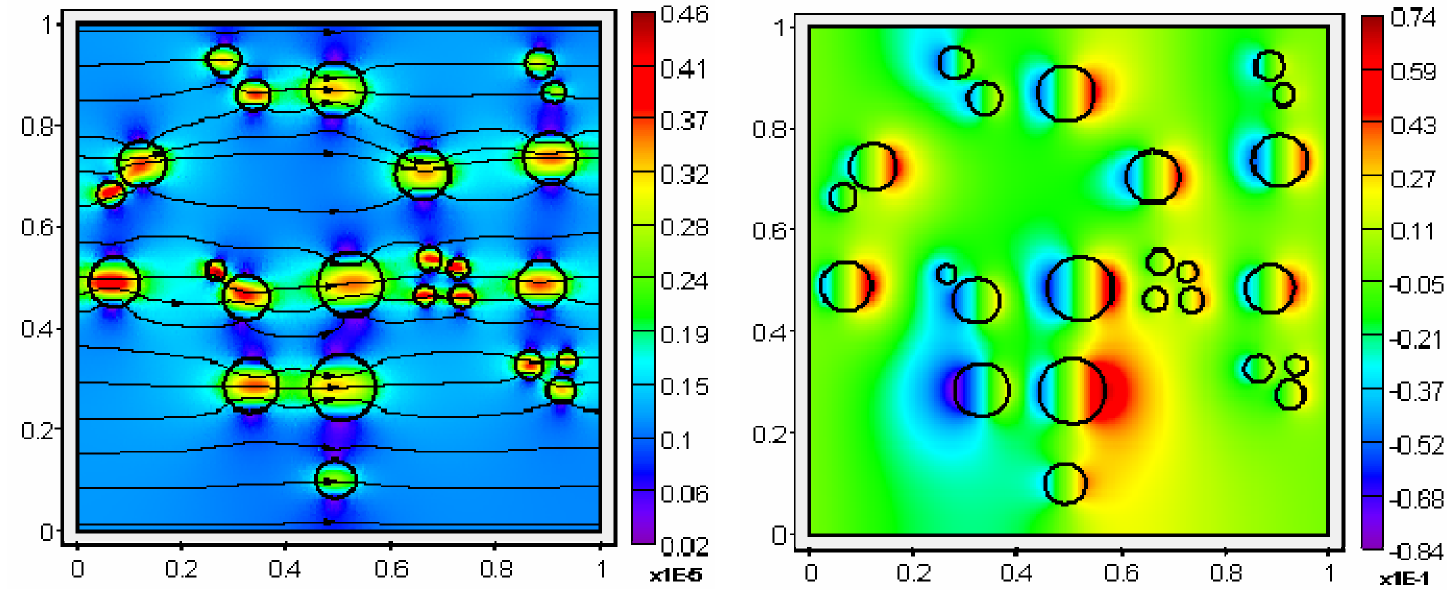

Velocity Magnitude and streamlines | Variation in the pressure distribution

Figure 5. Relative elementary volume with homogenous permeability background.
Parameters: Isotropic permeability $\mathbf{k} = 10^{-9} m^2$, $\mu^* = \mu = 0.001 Pa \cdot s$.
Boundary conditions: No flow at top and bottom side ($\mathbf{u}_2 = 0$), zero Neumann for the fluid stress at the left and right side and unit body force in the x-direction.
Upscaled permeability: $\mathbf{k}_{11} = \mu \langle \mathbf{u}_1 \rangle = 1.275 * 10^{-9} m^2$, $\mathbf{k}_{12} = \mu \langle \mathbf{u}_2 \rangle = 5.16 * 10^{-12} m^2$.

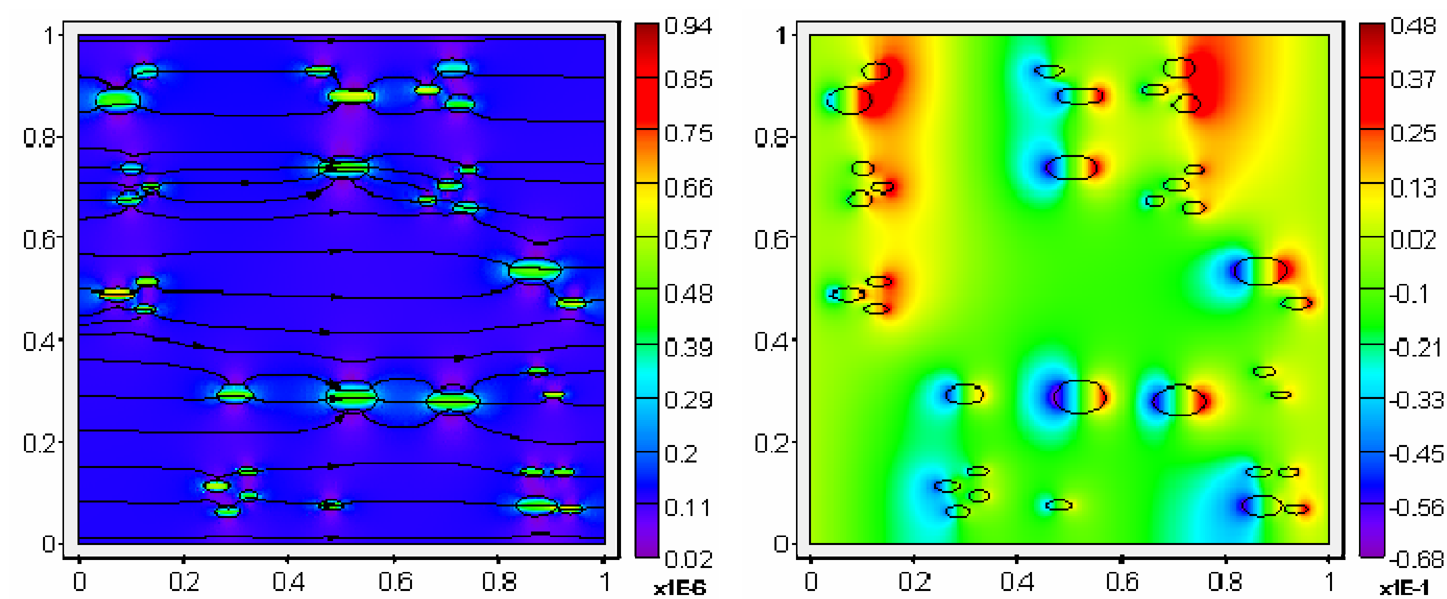

Velocity Magnitude and streamlines | Variation in the pressure distribution (after subtracting 1-x)

Figure 6. Velocity and pressure in vugular domain with homogeneous permeability background (5x5 coarsening will be performed).
Parameters: Isotropic permeability $\mathbf{k} = 10^{-10} m^2$, $\mu^* = \mu = 0.001 Pa \cdot s$.
Boundary conditions: No flow at top and bottom side ($\mathbf{u}_2 = 0$), zero Neumann for the fluid stress at the left and right side and unit body force in the x-direction.
Upscaled permeability (for the entire domain): $\mathbf{k}_{11} = \mu \langle \mathbf{u}_1 \rangle = 1.159 * 10^{-10} m^2$, $\mathbf{k}_{12} = \mu \langle \mathbf{u}_2 \rangle = -2.124 * 10^{-12} m^2$.

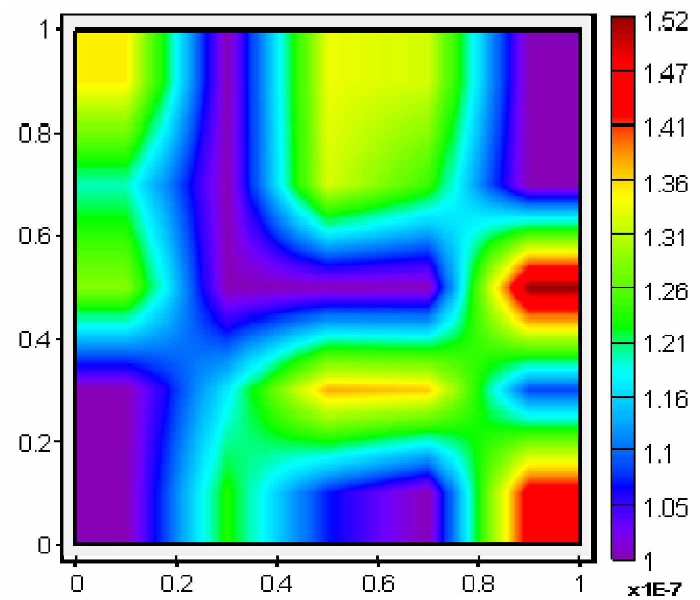

Figure 7. Homogenized absolute permeability field ($\mathbf{k}_{11}/\mu$). The values are computed by splitting the domain into 5x5 cells and solving two cell problems per cell. The cell problems are set up with periodic boundary conditions and unit force in the x-direction (to obtain $\mathbf{k}_{11}$) and y-direction (to obtain $\mathbf{k}_{22}$, not shown). The permability values are then placed at the cell centers and interpolated across the domain by bilinear interpolation.

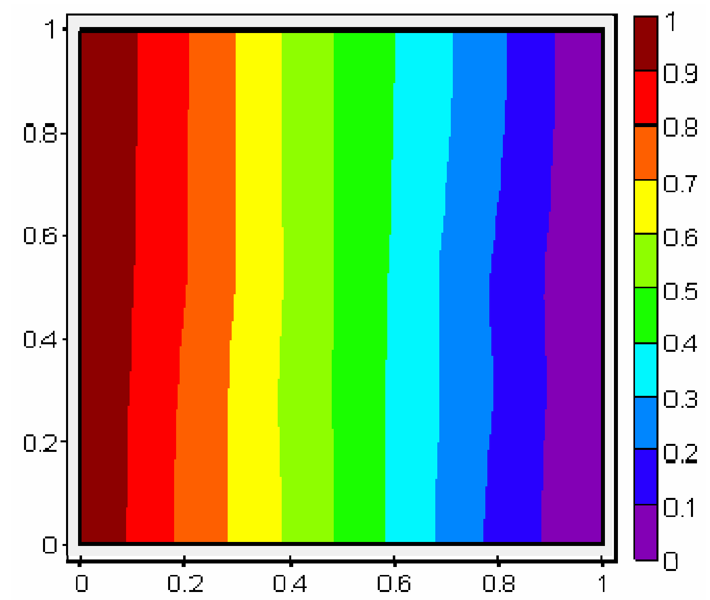

Figure 8. Coarse scale solution for the pressure.
Boundary conditions: $p = 1$ at the left side, $p = 0$ at the right side and zero Neumann at the top and bottom sides. The permeability field is a diagonal tensor with $\mathbf{k}_{11}$ and $\mathbf{k}_{22}$ components. $\mathbf{k}_{11}$ is shown in Fig.7.

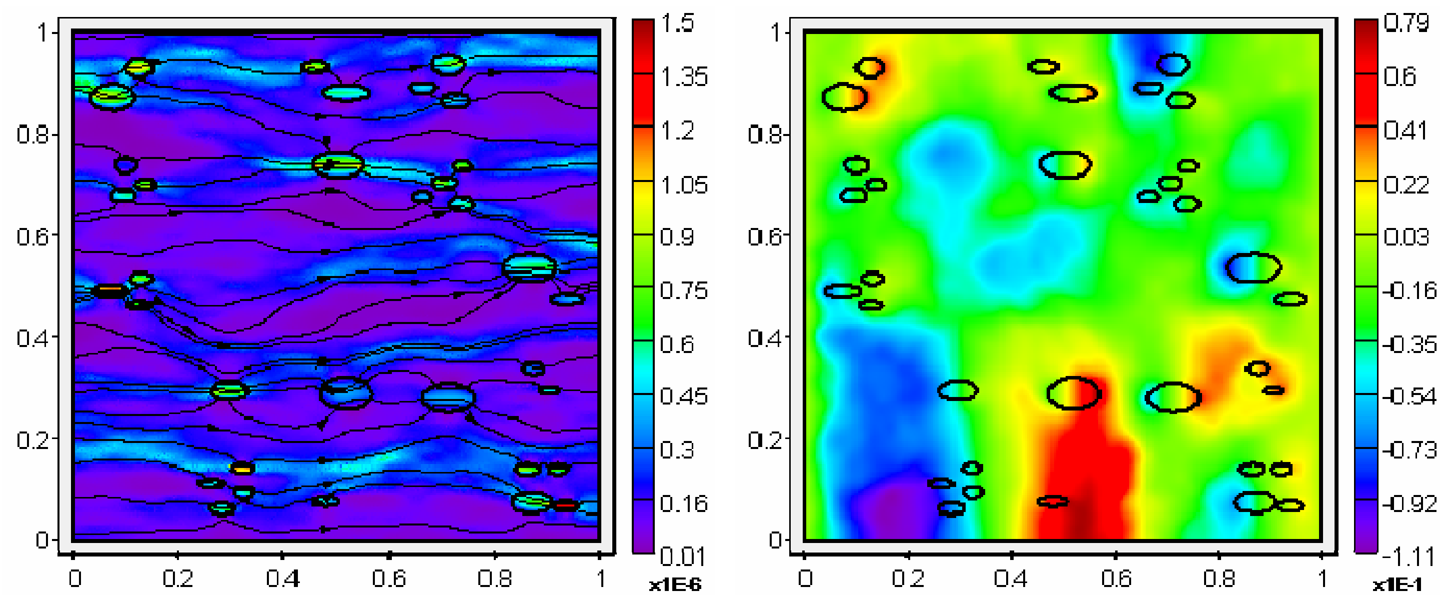

Velocity magnitude and streamlines

Variation in the pressure distribution (after subtracting 1-x)

Figure 9. Velocity and pressure in vugular domain with heterogeneous permeability background (5x5 coarsening will be performed).
Parameters: $\mathbf{k} = k\mathbf{I}$ is isotropic and variable (shown in Figure 10) with an average $\langle k \rangle = 10^{-10} m^2$, $\mu^* = \mu = 0.001 Pa \cdot s$.
Boundary conditions: No flow at top and bottom side ($\mathbf{u}_2 = 0$), zero Neumann for the fluid stress at the left and right side and unit body force in the x-direction.
Absolute upscaled permeability (for the entire domain): $\mathbf{k}_{11} = \mu \langle \mathbf{u}_1 \rangle = 1.566 * 10^{-10} m^2$, $\mathbf{k}_{12} = \mu \langle \mathbf{u}_2 \rangle = -1.838 * 10^{-12} m^2$

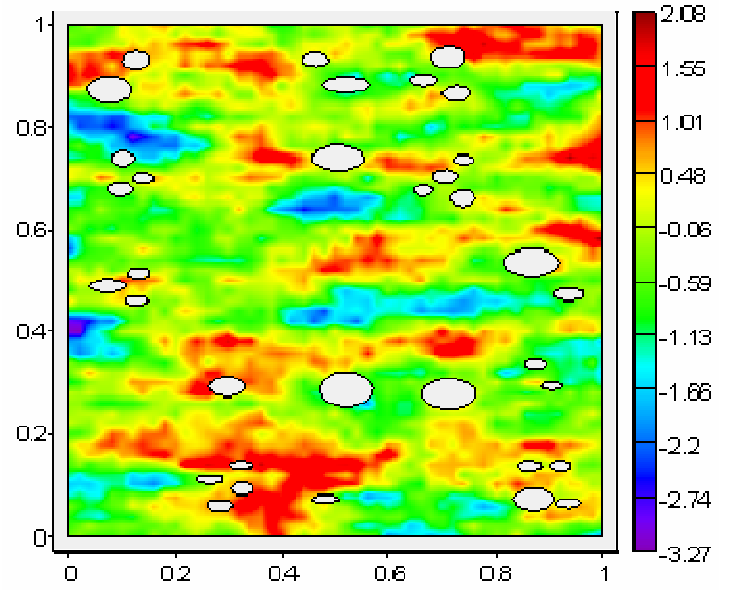

Figure 10. Log plot of the permeability field. The actual permeability used is $\mathbf{k} = C\exp(\cdot)\mathbf{I}$, where C is selected so that $\langle \mathbf{k} \rangle = 10^{-10} m^2$.

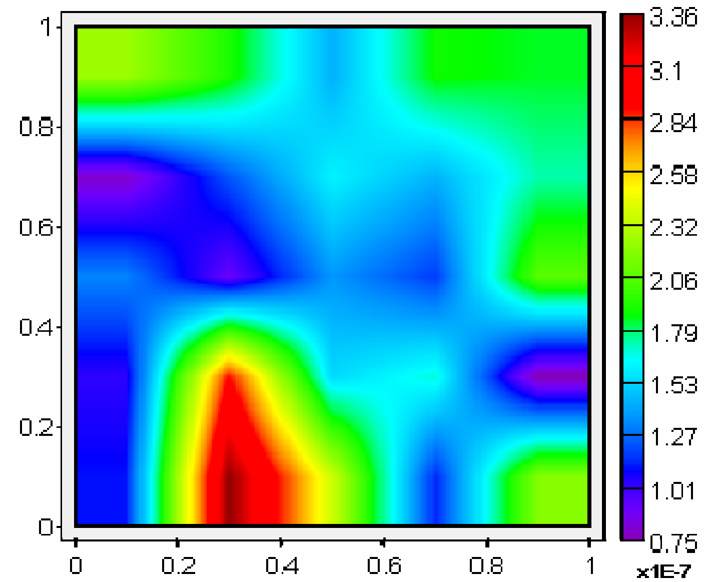

Figure 11. Homogenized absolute permeability field ($\mathbf{k}_{11}/\mu$). The values are computed by splitting the domain into 5x5 cells and solving two cell problems per cell. The cell problems are set up with periodic boundary conditions and unit force in the x-direction (to obtain $\mathbf{k}_{11}$) and y-direction (to obtain $\mathbf{k}_{22}$, not shown). The permability values are then placed at the cell centers and interpolated across the domain by bilinear interpolation.

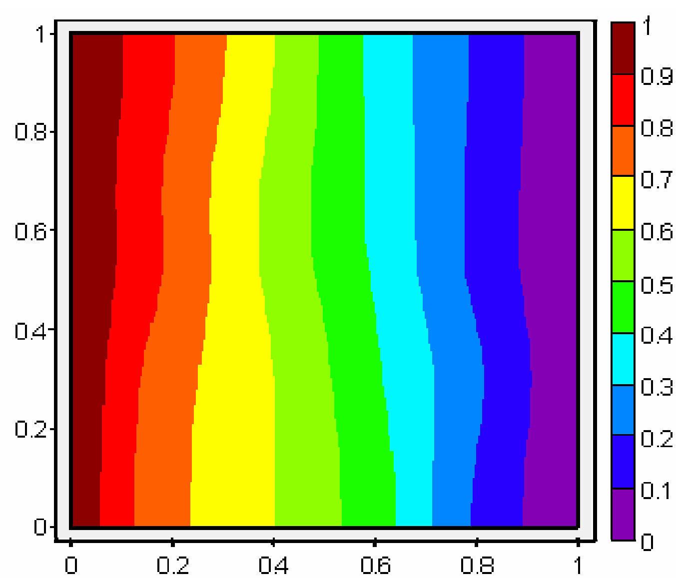

Figure 12. Coarse scale solution for the pressure.

Boundary conditions: $p = 1$ at the left side, $p = 0$ at the right side and zero Neumann at the top and bottom side. The permeability field is a diagonal tensor with $\mathbf{k}_{11}$ and $\mathbf{k}_{22}$ components. $\mathbf{k}_{11}$ is shown in Fig.10.